Sequential Detection of Unknown Frequency-Hopped Waveforms

WILLIAM E. SNELLING AND EVAGGELOS GERANIOTIS, SENIOR MEMBER, IEEE

Abstract—**The channelized receiver, which is optimal for the detection of unknown noncoherent frequency-hopped waveforms, bases its decision on a fixed-length block of input data. In this paper we present a sequential method of interception according to which, whenever a new data element is collected, a decision is made as to the presence or nonpresence of a frequency-hopped waveform. If that decision was indeterminate, another data element is collected. An optimal sequential test is derived, under the assumption that the waveform signal-to-noise ratio (S/N) is known. It is shown that this sequential test requires less data, on average, than the fixed length method to make a decision with the same reliability.**

A truncated sequential test is also derived where a decision is forced, if still indeterminate, after some fixed amount of data is collected. The truncated test is shown to improve the number of samples needed for a decision when the input signal-to-noise ratio differs greatly from that assumed in the derivation of the test. Furthermore, it is shown that the truncated test yields a limited degree of robustness when the input S/N differs from that assumed. A detailed analysis of the performance of these tests is conducted from which a method for finding an optimal truncation point follows. Numerical results which are based on this analysis, as well as on simulation of the interceptor's performance, are presented to prove the preceding statements.

I. Background and Introduction

THE first task in the interception of Spread Spectrum (SS) communications is the detection of the presence or nonpresence of the SS waveform to be intercepted. The detection of the SS waveform is a prelude to other interception processes such as feature detection, channel tracking, and message extraction. As a new development toward the detection problem, this paper applies and extends previously published results in sequential detection to the problem of the optimal detection of noncoherent Frequency-Hopped (FH) waveforms. By using likelihood function methods, the problem was previously solved in [2] for the case of an FH waveform with a known signal-to-noise ratio (SNR) and epochs with known starting times and durations. However, in that approach, the decision was based on a data segment of fixed size. Here, a sequential approach is taken, meaning that whenever a new data element is collected, a decision is attempted as to the presence or nonpresence of an FH waveform. If no decision is reached, another data element is collected.

The sequential approach to detection has a rich history. For the binary hypothesis problem with discrete-time independent identically distributed (i.i.d.) data, Wald [3] has derived the optimal sequential test. This test is optimal in the sense that no other test can reach a decision of the same Neyman–Pearson reliability within a smaller average time. This result has been extended to continuous time data in [4] and [5]. Others have suggested tests that must make a decision within a prescribed time. These are the "truncated" tests given in [6]–[8]. Truncation is desirable not only for implementation reasons but to improve the performance of a sequential test when the input statistics differ from those assumed in designing the test. In particular, Tantaratana and Poor [7] derived a truncated sequential test for i.i.d. Gaussian data with an unknown mean, which forms the foundation for the results included in this paper.

The process of development of the sequential test is begun by defining the observations model for a composite hypothesis problem. Specifically, given the observation $y(t)$, the problem is one of choosing between H_0, which is the hypothesis that an FH waveform is not present, and $H_{\gamma'}$, which is the hypothesis that an FH waveform is present with an SNR γ' where $0 < \gamma'$. The model is precisely

$$H_0\colon y(t) = n(t)$$

versus

$$H_{\gamma'}\colon y(t) = \sum_{i=1}^{N_h} x_i(t) + n(t) \qquad 0 < \gamma' \quad (1)$$

where

- $x_i(t)$ equals $\sqrt{2S'}\sin(\omega_{k_i}t + \theta_i)$ for $iT_h \le t \le (i+1)T_h$.
- $n(t)$ is white Gaussian noise with two sided spectral density $N_0/2$.
- ω_{k_i} for $1 \le k_i \le K$, is one of a family of known frequencies within the spread spectrum bandwidth with these being uniformly random for each epoch.
- θ_i is random phase with uniform distribution.
- S' is the average signal energy.
- T_h is the epoch, or time duration, of each hop.
- N_h is the number of hops over message duration.

Manuscript received August 1, 1988; revised January 15, 1989. This work was supported in part by Contel/Federal Systems Division through collaboration with the Systems Research Center at the University of Maryland.

W. E. Snelling is with the Johns Hopkins University, Applied Physics Laboratory, Johns Hopkins Rd., Laurel, MD 20707, and the Department of Electrical Engineering, University of Maryland, College Park, MD 20742.

E. Geraniotis is with the Department of Electrical Engineering and the Systems Research Center, University of Maryland, College Park, MD 20742.

IEEE Log Number 8927187.

The hypothesized SNR γ' is related to the other model parameters by

$$\gamma' = \frac{S' T_h}{N_0}. \tag{2}$$

Because a reliable test cannot be devised for FH waveform with an arbitrarily small SNR, the preceding composite hypothesis problem is simplified to a binary hypothesis problem: H_0 versus H_γ where γ is specified as the smallest SNR that is to be accurately detected. The quantity γ has the value

$$\gamma = \frac{S T_h}{N_0} \tag{3}$$

with S being the corresponding signal energy. The relative SNR $r = \sqrt{\gamma'/\gamma}$ will also be used.

Using the above observations model, the design of a sequential test for the detection of FH signals will be approached as follows. An asymptotically optical test will be derived by applying likelihood function theory to the simplified binary hypothesis problem: H_0 versus $H\gamma$. The parameters of this test will be specified to ensure a maximum probability of detection for a given probability of false alarm. This binary hypothesis test will then be applied to the more general composite hypothesis problem with a resulting degradation in detection time that will be shown to be controllable by properly truncating the test procedure.

The derivation of the asymptotically optimal test will begin with the derivation of the likelihood function for a single-epoch observation which is appropriately called the Single-Epoch Likelihood Function (SELF). Next, by invoking the central limit theorem, Gaussian densities will be found that are asymptotic to the actual SELF densities as the number of frequencies becomes large. In determining these densities, the SELF's means and variances will be explicitly computed under each hypothesis. By next considering individual SELF's as the observations, the problem will be reduced to a binary hypothesis problem with Gaussian i.i.d. observations. This simplification will be justified because each epoch of FH waveform has independent statistics and because the SELF's statistics do not depend on the particular hop frequency. Using these equivalent observations and their asymptotic densities, the Asymptotic Log Likelihood Function (ALLF) will be derived. The ALLF will then be used to synthesize tests for the binary hypothesis problem. This procedure will require extending the previously published sequential tests to the cases of data with variances which depend on the hypothesis. Applying these results, a Fixed-Sample Size (FSS) test, a Sequential Probability Ratio Test (SPRT), and a Truncated Sequential Test (TST) will be designed.

Each of the three tests will be analyzed by approximating the test statistic by a Wiener process and then employing the classical theory of diffusion as outlined in [5] and [6]. This analysis will be more general than that used to design the tests in that it will allow the performance of each test to be evaluated for the composite hypothesis problem rather than the assumed binary hypothesis problem. This analysis will yield the average decision time of each test as a function of the input SNR and will yield the operating characteristic of each test. From these results, an optimal test will be designed whose worst-case, average decision time is minimum. Finally, a computer simulation will confirm these analytical results.

To further extend these results to the case of a test that was synthesized under the expectation of detecting an FH waveform with extremely small SNR, an asymptotic analysis of a different sort will be undertaken. This analysis will show how the above tests perform for the composite hypothesis problem as the minimum reliably detectable SNR of the FH waveform becomes increasingly small. Numerical results for this case will be given, but a corresponding computer simulation is not possible due to the rate of increase of the number of computations required as the SNR diminishes.

II. Likelihood Function: One Epoch

The statistical test for the composite hypothesis problem is defined by finding an asymptotically optimal test for a binary hypothesis problem and applying that test to the composite case and accepting the resulting degradation. This simplified binary problem consists of the two hypotheses: H_0 where no signal is present, and H_γ where a signal is present with SNR γ. For this binary hypothesis problem, Appendix A contains a derivation of the SELF which is the likelihood function Λ_i of the ith-epoch observation $y(t)$ for $iT_h < t \leq (i+1)T_h$. The SELF is expressed as

$$\Lambda_i(y) \triangleq E_k[\Lambda_i(y/k)] \tag{4}$$

$$= \frac{e^{-\gamma}}{K} \sum_{k=0}^{K-1} I_0\left(\sqrt{2\gamma}\sqrt{P_k^2 + Q_k^2}\right) \tag{5}$$

where I_0 is the zeroth-order modified Bessel function of the first kind and

$$P_k = \frac{2}{\sqrt{N_0 T_h}} \int_{iT_h}^{(i+1)T_h} y(t) \cos \omega_{k_i} t \, dt$$

$$Q_k = \frac{2}{\sqrt{N_0 T_h}} \int_{iT_h}^{(i+1)T_h} y(t) \sin \omega_{k_i} t \, dt. \tag{6}$$

Because of the statistical independence between their respective observations, the likelihood function of the n-epoch observation is then $\Pi_{i=1}^{n} \Lambda_i$, i.e., the product of these individual SELF's.

The SELF is nicely modeled as the configuration of well-known devices as indicated in Fig. 1. That is, the SELF is channelized where each channel has a matched filter that is tuned to a particular hop frequency and whose output is envelope-detected and emphasized by a Bessel function nonlinearity. The output of each channel, after scaling by $e^{-\gamma}/K$, is summed up to produce the SELF.

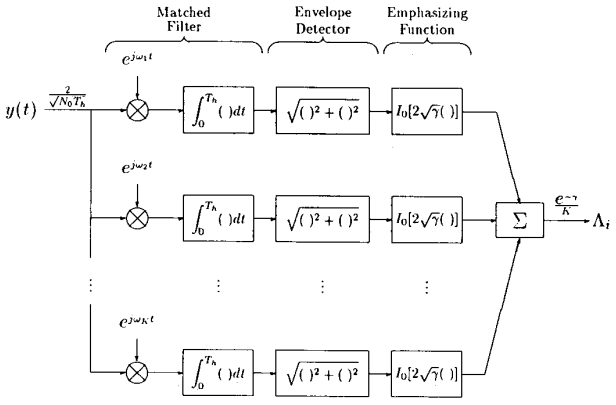

Fig. 1. Block diagram of single-epoch likelihood function.

III. Asymptotic Log-Likelihood Function

The Asymptotic Log-Likelihood Function (ALLF) is asymptotic to the n-epoch likelihood function, $\Pi_{i=1}^{n} \Lambda_i$, as the number of FH channels becomes large. The critical idea behind the derivation of the ALLF is the application of the central limit theorem to yield asymptotic densities for the SELF from which, using an n-epoch collection of SELF's as an equivalent observation set, the ALLF will be determined.

The SELF (5) was computed assuming a binary hypothesis problem, i.e., H_0 is the hypothesis that no FH waveform is present, while H_γ is the hypothesis that an FH waveform exists with a known SNR γ. The following analysis will assume that an FH waveform, if present, will have an SNR γ' or, equivalently, an average signal energy S' that is not necessarily equal to the average signal energy S assumed known in the binary case. This generalization is not necessary to derive the ALLF but will be needed to analyze the performance of the ALLF in the composite hypothesis problem.

Proceeding with the derivation of the ALLF, the central limit theorem is applied to the SELF to obtain an asymptotic density under all hypotheses, $0 \le \gamma'$. The central limit theorem is justified here because the SELF's output is the sum of many channels whose statistics will be shown to be nearly independent and nearly identical. It will be shown that the degree of dependence between channels is determined by the amount of isolation between channels which, in the case assumed here, is shown to be perfect for minimally spaced channels. It will also be shown that the channel means and variances, while different for the signal-present and signal-absent cases, are of a commensurate magnitude.

A. Matched Filter Output Statistics

Because the central limit theorem requires only the mean and variance of each channel, only the statistics of the matched filter outputs need to be determined exactly, since the SELF's mean and variances can be determined from these statistics alone. Assuming the signal present is in the kth channel, then the matched filter output in the lth channel can be found from (6) as

$$P_l \approx \begin{cases} \sqrt{2\gamma'} \sin\theta + \nu_l & \text{for } l = k \\ \nu_l & \text{for } l \neq k \end{cases} \tag{7}$$

$$Q_l \approx \begin{cases} \sqrt{2\gamma'} \cos\theta + \xi_l & \text{for } l = k \\ \xi_l & \text{for } l \neq k \end{cases} \tag{8}$$

where

$$\nu_l \triangleq \frac{2}{\sqrt{N_0 T_h}} \int_{iT_h}^{(i+1)T_h} n(t) \cos \omega_l t \, dt$$

$$\xi_l \triangleq \frac{2}{\sqrt{N_0 T_h}} \int_{iT_h}^{(i+1)T_h} n(t) \sin \omega_l t \, dt. \tag{9}$$

The matched filter outputs for the no-signal-present hypothesis H_0 are the special case of the above expressions for $\gamma' = 0$. Two assumptions were made in determining these approximate expressions for the matched filter outputs. The first assumption is that $\omega_k T_h$ is large and is equivalent to requiring a large number of carrier cycles over a single epoch. The second assumption of orthogonally spaced channels (i.e., $(\omega_k - \omega_l)T_h/2\pi$ is an integer) implies, in essence, that the channels are isolated from one another. Another condition implying channel isolation is wide spacing between the channels (i.e., $(\omega_k - \omega_l)T_h$ is large). In a practical implementation, smooth window functions could also have been used in the matched filter implementation to achieve the channel isolation assumed here.

Simplified expressions for the matched filter outputs are represented by (7) and (8). The statistical nature of their noise components, $\{\nu_l\}$ and $\{\xi_l\}$, will be determined next. From (9), it follows that the random variables $\{\nu_l\}$, $\{\xi_l\}$ are Gaussian with zero mean and unity variance. Under the isolated channel assumption, it is easy to show that

$$\begin{aligned} E[\nu_m \nu_n] &= 0 \quad \text{for } m \neq n \quad 1 \le m, n \le K \\ E[\nu_m \xi_n] &= 0 \quad \text{for all } m, n \quad 1 \le m, n \le K \\ E[\xi_m \xi_n] &= 0 \quad \text{for } m \neq n \quad 1 \le m, n \le K. \end{aligned} \tag{10}$$

Thus, $\{\nu_l\}$, $\{\xi_l\}$ are mutually independent, since they are Gaussian. These relations also determine the joint density of ν_l and ξ_l as

$$p_{\nu_l,\xi_l}(\nu_l, \xi_l) = \frac{1}{2\pi} e^{-(1/2)(\nu_l^2+\xi_l^2)}. \tag{11}$$

The equations (7), (8), and (10), along with the joint density of ν_l and ξ_l of (11), constitute a complete statistical description of the matched filter outputs $\{P_l\}$ and $\{Q_l\}$.

B. SELF Moments

The statistics of $\{P_l\}$ and $\{Q_l\}$ are used in determining the mean and variance of the SELF (5). The SELF moments are needed to apply the central limit theorem and thus ultimately produce the ALLF. A few conditions for

the application of the central limit theorem will be established now. First, since the random variables $\{P_l\}$ and $\{Q_l\}$ are mutually independent, each channel output of the SELF is also independent. Furthermore, the channel outputs are all identically distributed except for the output of the channel with the signal present. This particular channel output will be shown to have a variance comparable to that of the other channel outputs, in which case the central limit theorem still applies, providing us with a density asymptotic to the actual SELF density.

Subsequently, we need explicit expressions for the mean and variance of the SELF. Assuming a signal is present with a relative SNR of $r = \sqrt{\gamma'/\gamma}$, then the matched filter outputs of the channel containing the signal are by (7) and (8)

$$P_l = \sqrt{2\gamma'} \sin\theta + \nu_l$$
$$Q_l = \sqrt{2\gamma'} \cos\theta + \xi_l. \tag{12}$$

If μ_r and σ_r^2 are defined to be the mean and variance for this channel output, then (11) implies

$$\mu_r = E\left[I_0\left(\sqrt{2\gamma}\sqrt{P_l^2 + Q_l^2}\right)\right] \tag{13}$$
$$= \frac{1}{2\pi}\int_{-\infty}^{\infty}\int_{-\infty}^{\infty} I_0\left(\sqrt{2\gamma}\sqrt{P_l^2 + Q_l^2}\right) \cdot e^{-(1/2)(\nu_l^2+\xi_l^2)}\, d\nu_l\, d\xi_l. \tag{14}$$

Applying the rectangular-to-polar conversion, $P_l = \rho\cos\phi$, $Q_l = \rho\sin\phi$, and the identity

$$I_0(a) = \frac{1}{2\pi}\int_0^{2\pi} e^{a\cos\phi}\, d\phi \tag{15}$$

the integral becomes

$$\mu_r = e^{-\gamma'}\int_0^{\infty} \rho I_0\left(\sqrt{2\gamma}\rho\right) I_0\left(\sqrt{2\gamma'}\rho\right) e^{-(\rho^2/2)}\, d\rho \tag{16}$$
$$= e^{\gamma} I_0\left(2\sqrt{\gamma\gamma'}\right). \tag{17}$$

This integral was evaluated in [9, Section 13.31(1)]. The variance is now evaluated as follows:

$$\sigma_r^2 + \mu_r^2 = E\left[I_0^2\left(\sqrt{2\gamma}\sqrt{P_l^2 + Q_l^2}\right)\right] \tag{18}$$
$$= \frac{1}{2\pi}\int_{-\infty}^{\infty}\int_{-\infty}^{\infty} I_0^2\left(\sqrt{2\gamma}\sqrt{P_l^2 + Q_l^2}\right) \cdot e^{-(1/2)(\nu_l^2+\xi_l^2)}\, d\nu_l\, d\xi_l \tag{19}$$

which, by applying rectangular-to-polar conversion and (15), becomes

$$\sigma_r^2 + \mu_r^2 = e^{-\gamma'}\int_0^{\infty} \rho I_0^2\left(\sqrt{2\gamma}\rho\right) I_0\left(\sqrt{2\gamma'}\rho\right) e^{-(\rho^2/2)}\, d\rho. \tag{20}$$

This integral is evaluated by applying a formula from [9, Section 11.41(16)] which states

$$\frac{1}{\pi}\int_0^{\pi} I_0\left(\sqrt{a^2 + b^2 - 2ab\cos\phi}\right) d\phi = I_0(a)\, I_0(b). \tag{21}$$

Application of this formula and an interchange of integrations reduces the integral (20) to a simpler integral solved in [9, Section 13.31(1)]. The net result is

$$\sigma_r^2 + \mu_r^2 = \frac{e^{2\gamma}}{\pi}\int_0^{\pi} e^{-2\gamma\cos\phi} I_0\left(4\sqrt{\gamma\gamma'}\sin\frac{\phi}{2}\right) d\phi. \tag{22}$$

Summarizing, for a signal in channel l with an SNR γ', the channel moments are

$$\mu_r = e^{\gamma} I_0(2r\gamma)$$
$$\sigma_r^2 = e^{2\gamma}\left[\frac{1}{\pi}\int_0^{\pi} e^{-2\gamma\cos\phi} I_0\left(4r\gamma\sin\frac{\phi}{2}\right) d\phi - I_0^2(2r\gamma)\right] \tag{23}$$

where $r = \sqrt{\gamma'/\gamma}$.

The above calculations give expressions for the channel moments for a channel with a signal present. The moments for the case of a channel without a signal present are special cases of the above with $r = 0$, and are thus denoted by μ_0 and σ_0^2. From (23) and the Bessel function identity (15), they are

$$\mu_0 = e^{\gamma}$$
$$\sigma_0^2 = e^{2\gamma}\left[I_0(2\gamma) - 1\right]. \tag{24}$$

Likewise, moments for the lth channel, whenever it contains a signal with strength γ, correspond to the above moments with $r = 1$, and are thus denoted by μ_1 and σ_1^2.

As previously mentioned, the application of the central limit theorem depends on the various channel means and variances having commensurate amplitudes. The relative amplitudes between the moments are computed from (23) and (24) as

$$\frac{\mu_r}{\mu_0} = I_0(2r\gamma) \tag{25}$$

$$\frac{\sigma_r^2}{\sigma_0^2} = 1 + 2r^2\gamma + 2r^2\gamma^2 + \mathcal{O}(\gamma^3). \tag{26}$$

Hence, for small assumed SNR's ($\gamma \leq 1$), the mean and variance of the channel with a signal present and the mean and variance of the channels without a signal present are within a factor of three of each other.

Expressions for the mean and variance of the SELF can now be provided since the SELF is the sum of all K channels scaled by $e^{-\gamma}/K$. The expressions are

$$M_r = \frac{e^{-\gamma}}{K}\left[(K-1)\mu_0 + \mu_r\right] \tag{27}$$

$$V_r = \frac{e^{-2\gamma}}{K^2}\left[(K-1)\sigma_0^2 + \sigma_r^2\right]. \tag{28}$$

Here, M_r is the mean of the SELF when a signal of strength γ' is present, and M_0 and M_1 are written for the special cases of M_r when $r = 0$ and $r = 1$, respectively. The variances, V_r, V_0, and V_1, are defined similarly.

C. Derivation of the ALLF

With the first two moments of the SELF determined, the central limit theorem gives approximating densities to the SELF, Λ_i, under the composite hypothesis problem. These densities are

$$H_0\colon \Lambda_i \sim \frac{1}{\sqrt{2\pi V_0}} e^{-[(\Lambda_i - M_0)^2/2V_0]}$$

versus

$$H_{\gamma'}\colon \Lambda_i \sim \frac{1}{\sqrt{2\pi V_r}} e^{-[(\Lambda_i - M_r)^2/2V_r]} \qquad \text{for } 0 < \gamma' \leq \gamma \tag{29}$$

which gives a simplified statistical characterization of the SELF. That is, the SELF outputs, $\{\Lambda_i\}$, are Gaussian i.i.d. variables whose means and variances depend on the hypothesis.

In a procedure similar to deriving the SELF, the asymptotic log-likelihood function (ALLF) will be designed using the simpler binary hypothesis problem. For a single-epoch, likelihood function theory and (29) imply a log-likelihood function of

$$L_i(\Lambda_i) = c_2\Lambda_i^2 + c_1\Lambda_i + c_0 \tag{30}$$

where

$$c_2 = \frac{1}{2}\left(\frac{1}{V_0} - \frac{1}{V_1}\right) \tag{31}$$

$$c_1 = \left(\frac{M_1}{V_1} - \frac{M_0}{V_0}\right) \tag{32}$$

$$c_0 = \frac{1}{2}\left(\frac{M_0^2}{V_0} - \frac{M_1^2}{V_1} + \ln\frac{V_0}{V_1}\right). \tag{33}$$

Independence between observations over different epochs implies that the ALLF up to time n is

$$T_n = \sum_{i=1}^{n} L_i. \tag{34}$$

Now that ALLF has been found, its mean and variance will be computed as a prelude to investigating its performance in the composite hypothesis problem.

D. Moments of the ALLF

In the following, it is necessary to derive the moments of L_i from which the ALLF moments follow trivially from (34). Starting with the mean

$$\mathfrak{M}_r \triangleq E[L_i(\Lambda_i)] \tag{35}$$

$$= c_2E(\Lambda_i^2) + c_1E(\Lambda_i) + c_0 \tag{36}$$

$$= c_2(M_r^2 + V_r) + c_1M_r + c_0 \tag{37}$$

which expands in terms to the SELF moments to

$$\mathfrak{M}_r = \frac{1}{2}\ln\frac{V_0}{V_1} + (2V_1V_0)^{-1}[(M_r - M_0)^2V_1 - (M_r - M_1)^2V_0 + (V_1 - V_0)V_r]. \tag{38}$$

Now to compute the variance of L_i.

$$\mathfrak{V}_r = \text{Var}\,[L_i(\Lambda_i)] \tag{39}$$

which upon substitution of (30) yields

$$\mathfrak{V}_r = \text{Var}\,[c_2\Lambda_i^2 + c_1\Lambda_i + c_0]$$

$$= \text{Var}\,[(c_2M_r^2 + c_1M_r + c_0) \tag{40}$$

$$+ (2c_2M_r + c_1)v + c_2v^2] \tag{41}$$

where $v = \Lambda_i - M_r$. Furthermore,

$$\mathfrak{V}_r = \text{Var}\,[(2c_2M_r + c_1)v + c_2v^2] \tag{42}$$

$$= (2c_2M_r + c_1)^2V_r + 2c_2^2V_r^2 \tag{43}$$

which simplifies to

$$\mathfrak{V}_r = \frac{V_r^2}{2}\left(\frac{1}{V_0} - \frac{1}{V_1}\right)^2 + \left[\left(\frac{1}{V_0} - \frac{1}{V_1}\right)M_r + \left(\frac{M_1}{V_1} - \frac{M_0}{V_0}\right)\right]^2 V_r. \tag{44}$$

The special cases, $r = 1$ and $r = 0$, of the moments of L_i are, respectively, written as $\mathfrak{M}_1$ and $\mathfrak{M}_0$ for the means and as $\mathfrak{V}_1$ and $\mathfrak{V}_0$ for the variances.

E. Summary

A log-likelihood function for the binary hypothesis problem, designated as the ALLF, has been derived that is asymptotic to the true log-likelihood function as the number of channels becomes large. The ALLF was found with the help of likelihood function theory by considering an n-epoch collection of SELF's as a set of i.i.d. observations, assumed Gaussian by the central limit theorem. The Gaussian assumption was justified by showing that each SELF was the sum of nearly independent and nearly identical random variables. Various means and variances were also derived that will prove useful in the following. The ALLF will now be used to design an FSS test, SPRT, and a TST.

IV. Test Design

The results above reduced the problem of detecting an FH waveform to that of discriminating between two sets of Gaussian i.i.d. data with different means and variances. A Fixed Sample Size (FSS) test, a Sequential Probability Ratio Test (SPRT), and a Truncated Sequential Test (TST) based on this simplified model will be discussed.

A. FSS Test Design

As the name suggests, an FSS test consists of comparing a test statistic T_L, based on a fixed number L of observations, to a threshold τ. Then if the test statistic is greater than τ, the hypothesis H_1 is chosen while, correspondingly, a test statistic less than τ indicates hypothesis H_0. Symbolically this is

$$T_L \begin{cases} \geq \tau \Rightarrow H_1 \\ < \tau \Rightarrow H_0. \end{cases} \tag{45}$$

In our case, the test statistic is the L-epoch ALLF and the test parameters, L and τ, are specified to correspond to prescribed false alarm P_F and detection P_D probabilities. To determine L and τ, the density of the T_L is needed for each hypothesis. Although this density equals the noncentral χ^2 density, an approximate Gaussian density, derived via the central limit theorem, is used instead to yield simplified expressions for the test parameters. These densities are

$$H_0\colon T_L \sim \frac{1}{\sqrt{2\pi L \mathbb{V}_0}} e^{-[(T_L - L\mathfrak{M}_0)^2/2L\mathbb{V}_0]}$$

versus

$$H_1\colon T_L \sim \frac{1}{\sqrt{2\pi L \mathbb{V}_1}} e^{-[(T_L - L\mathfrak{M}_1)^2/2L\mathbb{V}_1]}. \tag{46}$$

From these densities, P_D and P_F can be computed in terms of L and τ to yield $P_F = 1 - \Phi(\tau - L\mathfrak{M}_0/\sqrt{L\mathbb{V}_0})$ and $P_D = 1 - \Phi(\tau - L\mathfrak{M}_1/\sqrt{L\mathbb{V}_1})$ where Φ^{-1} is the inverse of the distribution function of a zero mean, unity variance Gaussian random variable. These are solved simultaneously to provide

$$L = \frac{\left[\mathbb{V}_1^{1/2}\Phi^{-1}(1 - P_D) - \mathbb{V}_0^{1/2}\Phi^{-1}(1 - P_F)\right]^2}{(\mathfrak{M}_1 - \mathfrak{M}_0)^2} \tag{47}$$

$$\tau = \frac{L^{1/2}}{(\mathfrak{M}_1 - \mathfrak{M}_0)}\left[\mathbb{V}_0^{1/2}\mathfrak{M}_1\Phi^{-1}(1 - P_F) - \mathbb{V}_1^{1/2}\mathfrak{M}_0\Phi^{-1}(1 - P_D)\right]. \tag{48}$$

B. SPRT Design

Wald's sequential probability ratio test (SPRT) can now be defined as a test with test statistic T_n, based on n observations and two thresholds, a and b. The SPRT works as follows. Upon the nth observation, if T_n is greater than a, then the hypothesis H_1 is chosen. If T_n is less than b, then the hypothesis H_0 is chosen. If, instead, T_n is between a and b, the test statistic is updated to include $n + 1$ observations and the process is iterated. Symbolically this test is described as

$$\text{for each } n, \quad T_n \begin{cases} \geq a \Rightarrow H_1 \\ \leq b \Rightarrow H_0 \\ \in (a, b) \Rightarrow \text{take another sample.} \end{cases} \tag{49}$$

The threshold values, a and b, are assigned to give the desired Neyman–Pearson probability of detection P_D and probability of false alarm P_F. Relationships between the thresholds and the probabilities are given by Wald's approximations [3],

$$a \approx \ln\left(\frac{P_D}{P_F}\right) \tag{50}$$

$$b \approx \ln\left(\frac{1 - P_D}{1 - P_F}\right). \tag{51}$$

C. TST Design

Truncated Sequential Test (TST) is a hybrid of the above two tests. Specifically, TST follows the rules of a sequential test with test statistic T_n and with thresholds, a and b, but has the added feature of forcing a decision at time L (if no decision has yet been made) by comparing the test statistic to a threshold τ. Symbolically,

$$\text{for each } n < L, \quad T_n \begin{cases} \geq a \Rightarrow H_1 \\ \leq b \Rightarrow H_0 \\ \in (a, b) \Rightarrow \text{take another sample} \end{cases}$$

$$\text{but for } n = L, \quad T_L \begin{cases} \geq \tau \Rightarrow H_1 \\ < \tau \Rightarrow H_0. \end{cases} \tag{52}$$

Two relations secure the specification of the TST parameters, a, b, L, and τ. If P_F^* and P_D^* are the actual Neyman–Pearson probabilities for the TST, then from [7]

$$P_F^* \leq P_F^{FSS} + P_F^{SPRT} \tag{53}$$

$$(1 - P_D^*) \leq (1 - P_D^{FSS}) + (1 - P_D^{SPRT}) \tag{54}$$

where P_F^{FSS} is the probability of false alarm for the TST if $L = \infty$ and P_F^{SPRT} is the same probability for the TST if $a = -b = \infty$. P_D^{FSS} and P_D^{SPRT} are defined similarly. Thus, the errors of the TST can be viewed as a mixture of the errors of an FSS test with parameters L and τ, and an SPRT with parameters a and b. These inequalities can be verified by viewing ALLF, T_n, as a discrete stochastic process with time index n, and enumerating its sample paths. For instance, a sample path leading to a false alarm must either cross threshold a before threshold b and before time L, or be greater than threshold τ at time L. Since these events also correspond to false alarms in either the FSS test part or the SPRT part of the TST, the inequality (53) must follow.

The above inequalities can be used to specify a TST whose actual error probabilities, P_F^* and $1 - P_D^*$, are less than any specified error probabilities, P_F and $1 - P_D$. Thus, the TST can be designed by partitioning the bounding errors $(1 - P_D)$ and P_F among the SPRT and FSS test parts of the TST and then using the appropriate equation to compute the parameters L, τ, a, and b for TST [7]. Specifically, this partitioning is quantified with the introduction of two constants, $0 \leq C_1 \leq 1$ and $0 \leq C_2 \leq 1$, which are defined as TST mixture constants, with which the following can be constructed:

$$P_F^{FSS} = C_1 P_F \tag{55}$$

$$P_F^{SPRT} = (1 - C_1)P_F \tag{56}$$

$$(1 - P_D^{FSS}) = C_2(1 - P_D) \tag{57}$$

$$(1 - P_D^{SPRT}) = (1 - C_2)(1 - P_D) \tag{58}$$

for the error probabilities of the FSS test and SPRT parts of the TST. From the above inequalities and (47), (48), (50), and (51), the TST parameters are determined as fol-

lows:

$$L = \frac{\left[\mathcal{V}_1^{1/2}\Phi^{-1}(1 - P_D^{FSS}) - \mathcal{V}_0^{1/2}\Phi^{-1}(1 - P_F^{FSS})\right]^2}{(\mathfrak{M}_1 - \mathfrak{M}_0)^2} \tag{59}$$

$$\tau = \frac{L^{1/2}}{(\mathfrak{M}_1 - \mathfrak{M}_0)}\left[\mathcal{V}_0^{1/2}\mathfrak{M}_1\Phi^{-1}(1 - P_F^{FSS}) - \mathcal{V}_1^{1/2}\mathfrak{M}_0\Phi^{-1}(1 - P_D^{FSS})\right] \tag{60}$$

$$a = \ln\left(\frac{P_D^{SPRT}}{P_F^{SPRT}}\right) \tag{61}$$

$$b = \ln\left(\frac{1 - P_D^{SPRT}}{1 - P_F^{SPRT}}\right). \tag{62}$$

Note that (53) and (54) guarantee that the actual detection errors satisfy

$$P_F^* \leq P_F \tag{63}$$

$$1 - P_D^* \leq 1 - P_D. \tag{64}$$

The mixture constants, C_1 and C_2, reflect proportions of the FSS test and SPRT parts of the TST since if $C_1 = C_2 = 1$, a pure FSS test is defined, and if $C_1 = C_2 = 0$, a pure SPRT is defined. Criteria for choosing the mixture constants will be discussed in Section VI.

V. Performance of Tests

The problem addressed by the preceding tests—the FSS, the SPRT, and the TST—is the detection of the presence or nonpresence of an FH waveform. The detection of the FH waveform is a prelude to other interception processes such as feature detection, channel tracking, and message extraction. Here, the performance of the tests in detecting an FH waveform with variable amplitude and in the presence of white Gaussian noise is quantified.

The three tests were designed under the assumption of binary hypotheses. These hypotheses are H_0 (FH waveform is not present) and H_γ (FH waveform is present and has SNR γ). Of concern here is the performance of the three tests when the actual SNR γ' of the FH waveform satisfies $0 < \gamma' \leq \gamma$. Two parameters characterize a test's performance for a particular γ'. The first, denoted by $E(N/r, \gamma)$, is the Average Sample Number (ASN) which is defined as the average of the number of samples needed to reach a decision. The second parameter, denoted by $P_0(r, \gamma)$, is the Operating Characteristic (OC) which is defined as the probability of declaring the absence of an FH waveform. Both the ASN and OC are defined as functions of relative SNR r and the assumed SNR γ.

A. Analysis of FSS Test

For the FSS test, the ASN is obviously L, while the OC can be determined by approximating the ALLF at time L by a Gaussian random variable with the same moments. This central limit theorem argument produces

$$P_0(r, \gamma) = \Phi\left(\frac{\tau - L\mathfrak{M}_r}{\sqrt{L\mathcal{V}_r}}\right) \tag{65}$$

for the OC.

B. Analysis of SPRT

For the SPRT test, the analysis is more difficult but can be approached as a diffusion problem. Here, we approximate the test statistic by a Wiener process. Specifically, if $T(t)$ is a Wiener process with variance function $\mathcal{V}_r t$ and mean function $\mathfrak{M}_r t$, then the ALLF, T_n, converges weakly to $T(t)$ at integer times $t = n$ provided n is sufficiently large. This last restriction is needed to ensure that T_n has an approximate Gaussian density as implied by the central limit theorem. In terms of the approximating Wiener process $T(t)$, the problem of finding the OC function is now the problem of finding the probability that $T(t)$ will "touch" the lower threshold b before the upper threshold a. Likewise, the problem of finding the ASN is now the problem of finding the average time that $T(t)$ first "touches" either threshold (a or b). This time is also called the average stopping time. Expressions for these quantities are given in [5] and [6] as

$$P_0(r, \gamma) = \begin{cases} \dfrac{e^{-2b(\mathfrak{M}_r/\mathcal{V}_r)} - 1}{e^{-2b(\mathfrak{M}_r/\mathcal{V}_r)} - e^{-2a(\mathfrak{M}_r/\mathcal{V}_r)}} & \mathfrak{M}_r \neq 0 \\ \dfrac{a}{a - b} & \mathfrak{M}_r = 0 \end{cases} \tag{66}$$

$$E(N/r, \gamma) = \begin{cases} \dfrac{aP_0(r, \gamma) + b[1 - P_0(r, \gamma)]}{\mathfrak{M}_r} & \mathfrak{M}_r \neq 0 \\ -\dfrac{ab}{\mathcal{V}_r} & \mathfrak{M}_r = 0. \end{cases} \tag{67}$$

C. Analysis of TST

The diffusion analysis technique also applies to the TST but is more involved. The ASN is by [5]

$$E(N/r, \gamma) = A\sum_{n=1}^{\infty}(-1)^n\frac{n}{k_n^2}B_n(e^{-k_nL} - 1) \tag{68}$$

where

$$A = \frac{\mathcal{V}_r\pi}{(a - b)^2} \tag{69}$$

$$B_n = e^{\mathfrak{M}_r b/\mathcal{V}_r}\sin\frac{n\pi a}{a - b} - e^{\mathfrak{M}_r a/\mathcal{V}_r}\sin\frac{n\pi b}{a - b} \tag{70}$$

$$k_n = \frac{\mathfrak{M}_r^2}{2\mathcal{V}_r} + \frac{\mathcal{V}_r n^2\pi^2}{2(a - b)^2}. \tag{71}$$

The OC function defined is by [6] as

$$P_0(r, \gamma) = \Phi\left(\frac{\tau - L\mathfrak{M}_r}{\sqrt{L\mathfrak{V}_r}}\right) - \sum_{n=1}^{\infty} e^{2(\mathfrak{M}_r/\mathfrak{V}_r)[na-(n-1)b]} \Phi\left(\frac{\tau - L\mathfrak{M}_r - 2[na-(n-1)b]}{\sqrt{L\mathfrak{V}_r}}\right) + e^{2(\mathfrak{M}_r/\mathfrak{V}_r)n(a-b)}\Phi\left(\frac{\tau - L\mathfrak{M}_r - 2n(a-b)}{\sqrt{L\mathfrak{V}_r}}\right) + e^{2(\mathfrak{M}_r/\mathfrak{V}_r)[nb-(n-1)a]} \Phi\left(\frac{2[nb-(n-1)a] - \tau + L\mathfrak{M}_r}{\sqrt{L\mathfrak{V}_r}}\right) - e^{2(\mathfrak{M}_r/\mathfrak{V}_r)n(b-a)}\Phi\left(\frac{2n(b-a) - \tau + L\mathfrak{M}_r}{\sqrt{L\mathfrak{V}_r}}\right). \quad (72)$$

Equations (65)–(72) represent a complete characterization of the performance of the FSS test, SPRT, and TST.

The fact that the diffusion technique yields accurate expressions for the ASN and OC functions will not be proved here but will be verified below by computer simulations.

D. Numerical Results

The FSS test, SPRT, and TST were simulated to verify the assumptions of the analysis and as an independent measure of the relative performance of the three tests. The simulated detector consists of 512 channels, and each test was synthesized to ensure a probability of false alarm P_F of no more than 1 percent and a probability of detection P_D of at least 99 percent. Here, the fairly relaxed probability of false alarm of 1 percent was chosen in order to limit the amount of data needed for a decision. Under these specifications, the simulation was run until 1000 decisions were reached for each of 11 SNR's evenly spaced between 0 and γ. The decisions that no FH waveform was present were averaged to estimate the OC, while the number of observations taken to reach a decision were averaged to estimate the ASN. Additionally, the standard deviation of ASN average was measured to indicate the ASN estimation error.

Figs. 2 and 3 are, respectively, the ASN's by simulation and by theory when the assumed SNR $\gamma = 1$, while Figs. 4 and 5 are the corresponding curves for ($\gamma = 0.3$). As predicted, the ASN is reduced by about 57 percent, for the SPRT in the regions around $\gamma' = 0$ and $\gamma' = \gamma$. These curves exemplify a general property of the SPRT. That is, the SPRT performs very well when the observations statistics are close to those assumed, but the SPRT exhibits a degraded performance, often to the point of being worse than the FSS test, when the observations statistics are different. In our context, this degradation is evidenced by a large ASN for the SPRT when the actual S/N, γ', is midway between the two assumed values 0 and γ. The TST reduces the ASN in this mid-S/N region as shown by the figures, but it does this at the expense of performance in the regions around $\gamma' = 0$ and $\gamma' = \gamma$. Despite this performance loss, truncation is necessary for implementation reasons. It will also be shown that the TST has the desirable property of having a higher detection probability than the SPRT at small SNR's, and that through optimization of the mixture constants, the TST can regain much of what it lost in ASN around $\gamma' = 0$ and $\gamma' = \gamma$.

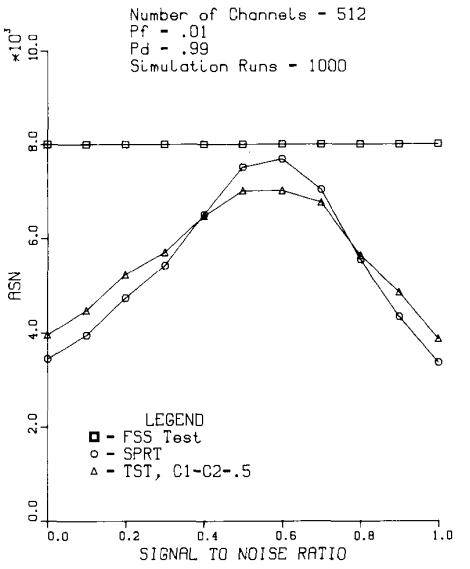

Fig. 2. ASN from simulation versus S/N, $\gamma = 1$.

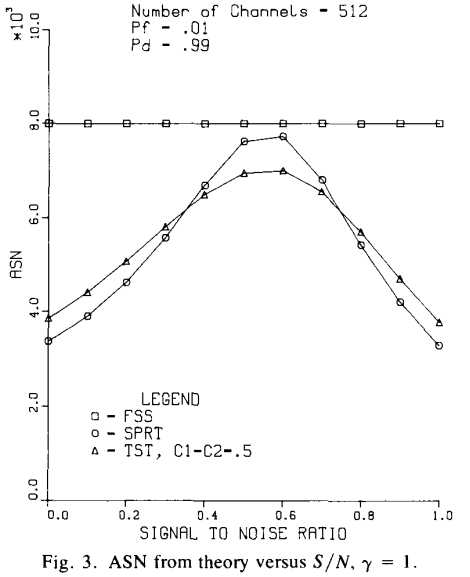

Fig. 3. ASN from theory versus S/N, $\gamma = 1$.

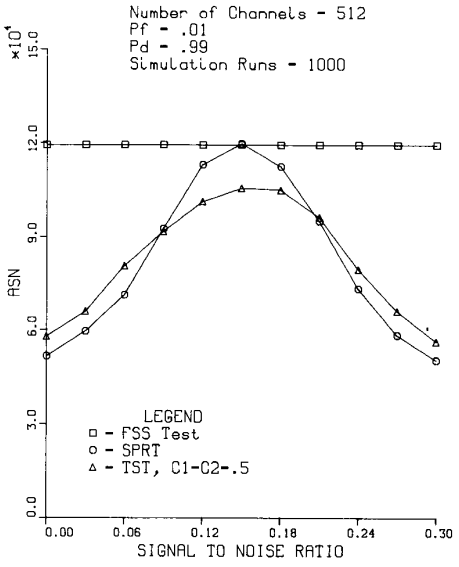

Fig. 4. ASN from simulation versus S/N, $\gamma = 0.3$.

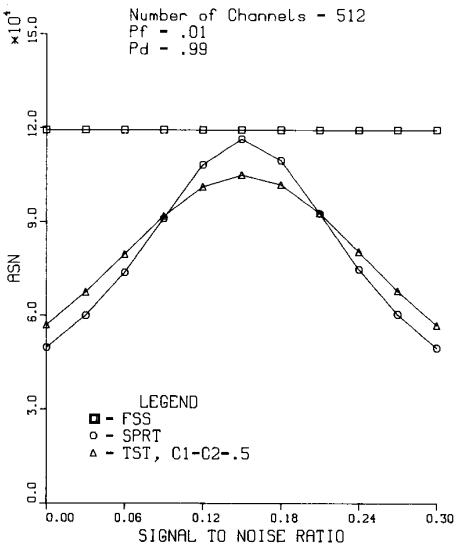

Fig. 5. ASN from theory versus S/N, $\gamma = 0.3$.

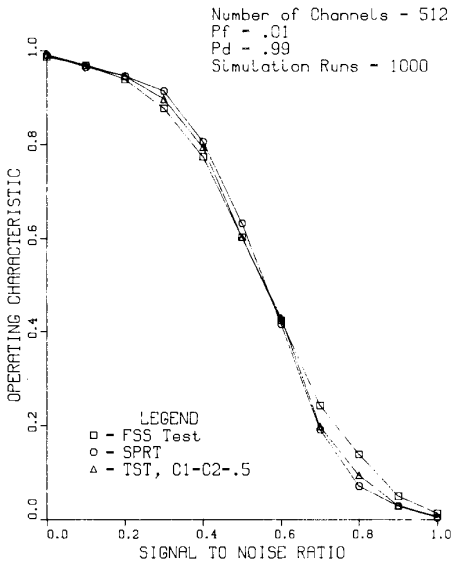

Fig. 6. OC from simulation, $\gamma = 1$.

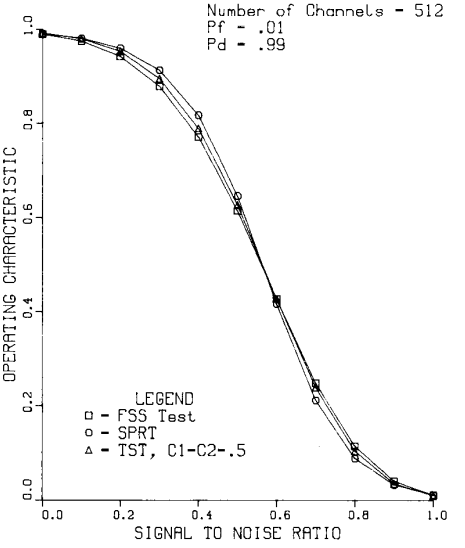

Fig. 7. OC from theory, $\gamma = 1$.

Focusing on the OC's (Figs. 6 and 7 for $\gamma = 1$, Figs. 8 and 9 for $\gamma = 0.3$), it is obvious that the FSS test has a slightly higher probability of detection for small SNR's while the SPRT has degraded performance in this region. Notice that these test performances are reversed for SNR's close to γ. The OC's also show that the TST's actual detection errors, P_F and $1 - P_D$, are within 79 percent of their specified bounds, P_F^* and $1 - P_D^*$.

Throughout the analysis, various simplifying approximations were made whose accuracies were hard to quantify, especially the Wiener process approximations to the ALLF. Thus, the computer simulation was compared quantitatively to results predicted by theory as a validation of assumptions made. Table I for $\gamma = 1$, and Table II for $\gamma = 0.3$, show how well the simulation of the three tests correspond to the analysis. The quantity ΔASN is the normalized difference between the theoretical ASN and the simulation ASN where the normalizing factor is the estimated standard deviation of the average used to estimate the ASN. The ΔASN values show a good correspondence between theory and simulation since they are within two standard deviations 86 percent of the time. The quantity ΔOC is the normalized difference between the theoretical OC and the simulation OC. Here, the normalizing factor is the standard deviation of the OC average assuming that the theoretical OC value is correct. In other words, the normalizing factor for a theoretical OC of $P_0(\gamma')$ and 1000 simulation runs is σ_{OC} =

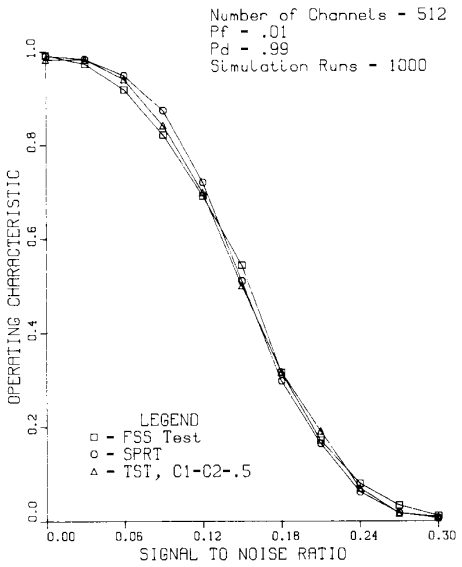

Fig. 8. OC from simulation, $\gamma = 0.3$.

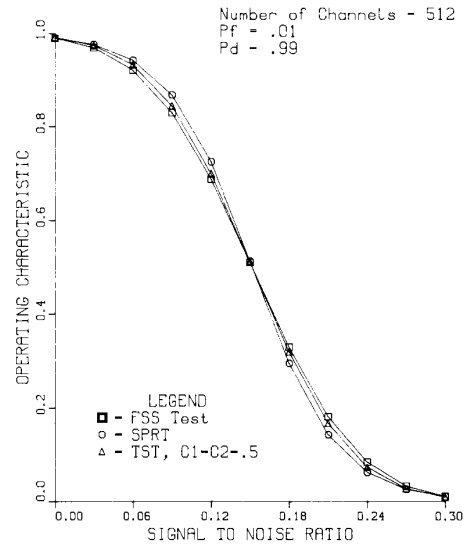

Fig. 9. OC from theory, $\gamma = 0.3$.

TABLE I
COMPARISON BETWEEN THEORY AND SIMULATION FOR $\gamma = 1$

γ'	FSS test		SPRT		TST	
	Δ ASN	Δ OC	Δ ASN	Δ OC	Δ ASN	Δ OC
0.00	0.00	0.84	-1.19	-0.03	-1.47	0.03
0.10	0.00	1.11	-0.48	2.77	-0.76	2.03
0.20	0.00	0.45	-1.05	1.92	-1.84	1.02
0.30	0.00	0.18	1.16	-0.09	1.19	-0.18
0.40	0.00	-0.25	1.09	0.89	0.20	-0.40
0.50	0.00	0.73	0.60	0.83	-0.64	1.53
0.60	0.00	0.22	0.23	0.02	-0.14	-0.15
0.70	0.00	0.37	-1.47	1.64	-2.35	3.20
0.80	0.00	-2.16	-0.94	2.25	0.76	1.17
0.90	0.00	-1.33	-1.38	0.83	-1.88	1.02
1.00	0.00	-0.84	-1.16	3.50	-1.38	1.29

TABLE II
COMPARISON BETWEEN THEORY AND SIMULATION FOR $\gamma = 0.3$

γ'	FSS test		SPRT		TST	
	Δ ASN	Δ OC	Δ ASN	Δ OC	Δ ASN	Δ OC
0.00	0.00	-0.71	-1.92	0.02	-1.04	2.09
0.03	0.00	-0.73	0.32	-1.75	1.38	-2.18
0.06	0.00	0.34	1.59	-0.82	-0.71	-1.03
0.09	0.00	0.68	-0.65	-0.49	0.07	0.28
0.12	0.00	-0.24	-1.72	0.33	-0.14	0.08
0.15	0.00	-2.17	-1.09	0.17	-0.48	0.69
0.18	0.00	0.91	-0.96	-0.19	-2.32	0.16
0.21	0.00	0.88	-1.04	-1.83	-2.49	-1.93
0.24	0.00	0.56	0.98	0.09	0.78	0.43
0.27	0.00	-0.18	1.79	2.02	1.70	2.68
0.30	0.00	-0.30	-0.70	1.67	0.63	0.20

$\sqrt{P_0(\gamma')[1 - P_0(\gamma')]/1000}$. Here again, in Tables I and II, a good correspondence between theory and simulation is apparent.

The purpose of the computer simulation was to validate the assumptions made in the specification and analysis of the three tests—the FSS test, SPRT, and TST. The accuracy with which the analysis predicts quantities measured by simulation, as shown above, substantiates fully the assumptions made.

VI. Test Extensions

The analytical expressions (68) for the ASN and (72) OC of the TST can be used to determine a TST with an optimum mixture of FSS and SPRT parts. Specifically, the maximum ASN with respect to the SNR γ' varies as a function of the mixture constants C_1 and C_2. This function is graphed in Fig. 10. The figure indicates that the optimal TST should have a greater mix of SPRT than the value one-half used in Section V since the maximum ASN of smallest value occurs for smaller values of the mixture constants, C_1 and C_2. The optimal mixture constants were found numerically to be $C_1 = 0.286$ and $C_2 = 0.284$. The ASN and OC of the optimal TST are shown in Figs. 11 and 12. It is interesting that by minimizing the maximum ASN, the ASN in the extreme regions about $\gamma' = 0$ and $\gamma' = \gamma$ is also reduced. This is believed to be a consequence of the optimal TST having a greater mix than the half-and-half arbitrarily picked for the Section V simulation and, therefore, exhibits properties closer to a pure SPRT. Of course, if the first TST was specified to have a larger SPRT mix, then optimization would have increased the ASN in the extreme regions. The optimal TST offers a good compromise between the need to maximize the ASN performance in the extreme regions and the need to minimize the maximum ASN.

Another extension to the previously described tests is the robustification of the tests with respect to the assumed SNR, γ. This can be accomplished by specifying the assumed SNR γ for the worst-case SNR for which detection is desired, and then choosing a corresponding minimum probability of detection P_D^* that is somewhat relaxed. This procedure produces a test that adequately detects over a

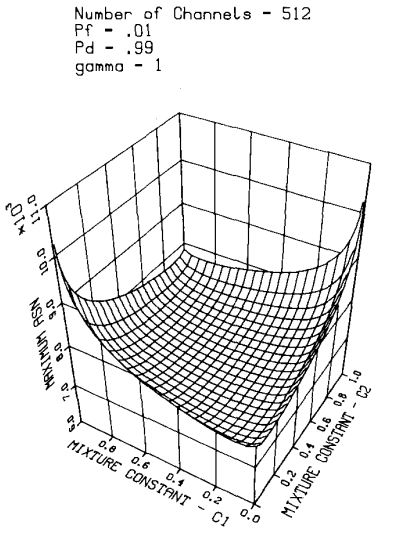

Fig. 10. Maximum ASN versus test mixture constants, C_1 and C_2.

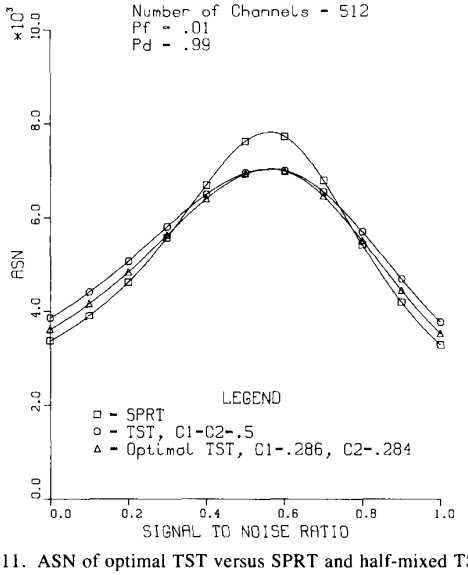

Fig. 11. ASN of optimal TST versus SPRT and half-mixed TST.

broader range of SNR's, and it is a way to effectively use the smaller detection times of the SPRT and TST. In this way, either a TST or SPRT can be designed that adequately detects over a broader range of SNR's than that of an FSS test with the same or greater detection time.

The described tests can also be extended to the slow FH case. The detector structure itself is optimal under the fast FH assumption, but is also a reasonable suboptimal structure for slow FH signals. This is especially true when there are a large number of hops over a given detection time. Even though the detector itself is suboptimal for slow FH, all the performance and design analyses developed for fast FH apply directly. This is because our design and performance analyses depended only on the chip duration being known and on the interference being additive white Gaussian noise.

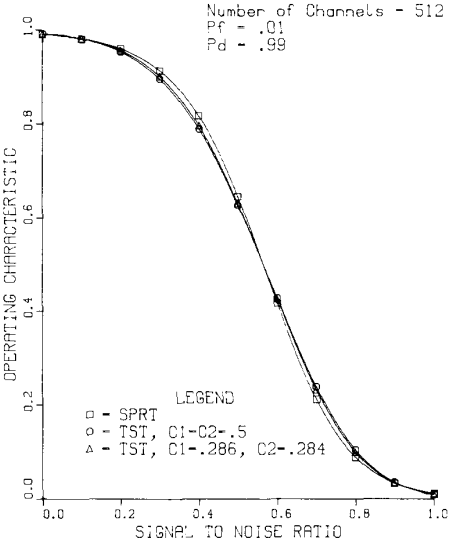

Fig. 12. OC of optimal TST versus SPRT and half-mixed TST.

VII. Asymptotic Efficiencies

The previous analysis did not include the performance of the tests when the assumed SNR γ is small. This case will be examined here. Since the ASN and OC are functions of both γ and the actual SNR γ', the ASN and OC can be recast as functions of γ and the relative SNR $r = \sqrt{\gamma'/\gamma}$. Test performance in the dwindling SNR case is captured by the limit of the ASN and OC as γ diminishes while r is held constant. For the OC, this is a finite limit, but the ASN increases without bound. Thus, rather than comparing the ASN's directly, the limit of the ASN times γ^2 is computed. In other words, a quantity, identified as the asymptotic ASN, $\tilde{E}(N/r)$, will be defined as

$$\tilde{E}(N/r) = \lim_{\gamma \to 0} \gamma^2 E(N/r, \gamma). \tag{73}$$

The asymptotic ASN is useful because it preserves the relative efficiencies between the ASN's as γ diminishes. For instance, consider the FSS test ASN, $E^{FSS}(N/r, \gamma)$, and the SPRT ASN, $E^{SPRT}(N/r, \gamma)$, and write

$$\lim_{\gamma \to 0} \frac{E^{FSS}(N/r, \gamma)}{E^{SPRT}(N/r, \gamma)} = \frac{\tilde{E}^{FSS}(N/r)}{\tilde{E}^{SPRT}(N/r)} \tag{74}$$

where $\tilde{E}^{FSS}(N/r)$ and $\tilde{E}^{SPRT}(N/r)$ are the asymptotic ASN's of the FSS test and SPRT, respectively. The asymptotic OC is simply defined as

$$\tilde{P}_0(r) = \lim_{\gamma \to 0} P_0(r, \gamma). \tag{75}$$

As an aid in evaluating these limits, we have asymptotic expressions for moments of the single-epoch ALLF derived in subsection B of the Appendix defined as follows:

$$\mathfrak{M}_r = \tilde{\mathfrak{M}}_r \gamma^2 + \mathcal{O}(\gamma^3) \tag{76}$$

$$\mathcal{V}_r = \tilde{\mathcal{V}}_r \gamma^2 + \mathcal{O}(\gamma^3) \tag{77}$$

where

$$\tilde{\mathfrak{M}}_r = \frac{K+2}{K^2}\left(r^2 - \frac{1}{2}\right) \tag{78}$$

$$\tilde{\mathfrak{V}}_r = \frac{K+2}{K^2}. \tag{79}$$

Here and throughout this discussion, the quantity $\mathcal{O}(\gamma^n)$ represents any function, say $f(\gamma)$, such that

$$\gamma^{-n} \lim_{\gamma \to 0} f(\gamma) < \infty. \tag{80}$$

The particular function represented by $\mathcal{O}(\gamma^n)$ is determined from the context of the equation in which it appears.

To ease the expression of the asymptotic ASN and asymptotic OC, the variables, $\tilde{L}$, $\tilde{r}$, $\tilde{a}$, and $\tilde{b}$ are defined. They will be labeled the asymptotic test parameters. Depending on the test type, they have expressions that correspond to that test type's parameter equations where $\mathfrak{M}_r$ is replaced with $\tilde{\mathfrak{M}}_r$, and likewise $\mathfrak{V}_r$ is replaced with $\tilde{\mathfrak{V}}_r$. For instance, the FSS asymptotic test parameters are from (47) and (48)

$$\tilde{L} = \frac{\left[\tilde{\mathfrak{V}}_1^{1/2}\Phi^{-1}(1-P_D) - \tilde{\mathfrak{V}}_0^{1/2}\Phi^{-1}(1-P_F)\right]^2}{\left(\tilde{\mathfrak{M}}_1 - \tilde{\mathfrak{M}}_0\right)^2} \tag{81}$$

$$\tilde{\tau} = \frac{\tilde{L}^{1/2}}{\left(\tilde{\mathfrak{M}}_1 - \tilde{\mathfrak{M}}_0\right)}\left[\tilde{\mathfrak{V}}_0^{1/2}\mathfrak{M}_1\Phi^{-1}(1-P_F) - \tilde{\mathfrak{V}}_1^{1/2}\tilde{\mathfrak{M}}_0\Phi^{-1}(1-P_D)\right]. \tag{82}$$

By using the asymptotic expressions (76) and (77), we have proved that the asymptotic ASN and OC of a particular test are exactly those of a test with the corresponding asymptotic test parameters. For example, this fact and (65) suggest that for the FSS test, the asymptotic ASN is

$$\tilde{E}^{FSS}(N/r) = \tilde{L} \tag{83}$$

while the FSS test's asymptotic OC is

$$\tilde{P}_0(r) = \Phi\left(\frac{\tilde{r} - \tilde{L}\tilde{\mathfrak{M}}_r}{\sqrt{\tilde{L}\tilde{\mathfrak{V}}_r}}\right). \tag{84}$$

The ASN and OC for the three different tests were plotted and compared in Figs. 13 and 14. The relative relationship between the tests' asymptotic ASN's is almost exactly like that between the ASN's for $\gamma = 1$ and $\gamma = 0.3$ shown in Figs. 2–5. This indicates that the three tests have already reached their asymptotes even for $\gamma = 1$. This comment also applies to the OC's. The usefulness of this asymptotic analysis, beyond verifying that the relationship between tests remain the same for diminishing SNR, is that it simplifies the test parameter relationships with respect to the parameters, γ and r. Thus, for each test, we could choose parameters: $L = \tilde{L}\gamma^{-2}$, $\tau = \tilde{\tau}$, $a = \tilde{a}$, and $b = \tilde{b}$, and still have comparable performance for any small γ. This feature simplifies any adaptation with respect to γ that might be added to this detection scheme.

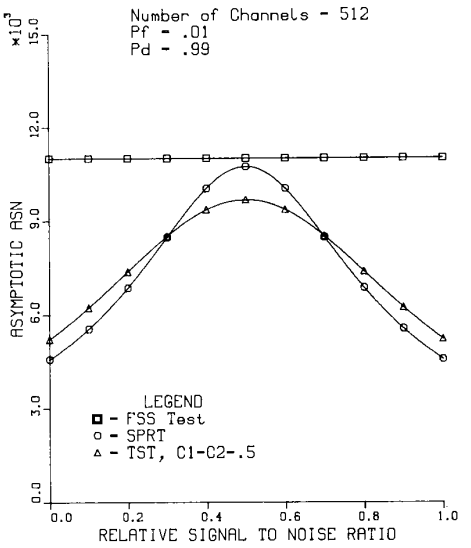

Fig. 13. Asymptotic ASN of FSS test, SPRT, and TST.

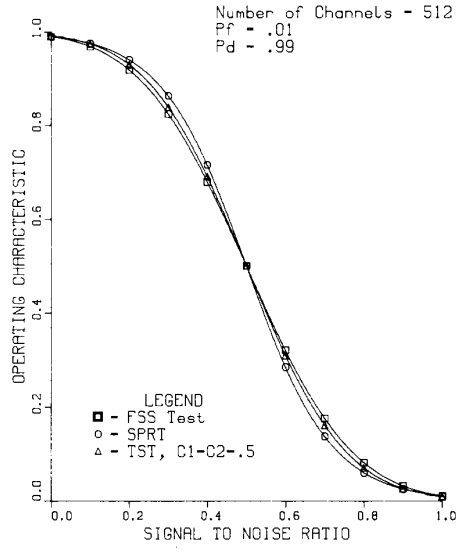

Fig. 14. Asymptotic OC function of FSS test, SPRT, and TST.

VIII. Conclusions

In this paper, methods for the detection of noncoherent fast FH waveforms have been developed. In the process, the FH waveform was modeled to have an information component which consisted of a series of chips with a known constant epoch where each chip frequency is one of a known ensemble of frequencies. In the model, a particular chip frequency is independently determined by a uniform random variable on the frequency ensemble. The FH waveform was also assumed to have an additive white noise component. By assuming the modeled FH waveform was of a known SNR, the optimal detector based on a single-epoch observation (SELF) was developed using likelihood-function theory. SELF was the sum of many identical and nearly independent random variables and

thus had nearly Gaussian statistics. This central limit argument allowed a multiepoch collection of SELF's to be considered an equivalent set of Gaussian i.i.d. variables. From these simplified observations, a log-likelihood function (ALLF) was computed that was asymptotic to the exact log-likelihood function as the number of possible hop frequencies becomes large. ALLF became the test statistic from which three detection tests were based. The tests were: the FSS test, SPRT, and TST. These were defined to ensure that detection errors were below desired levels. By modeling the ALLF as Wiener process, diffusion theory yielded not only the performance of the three tests for an FH waveform of the assumed SNR but also the test performance for all SNR's below the one assumed. This analysis compared favorably to a computer simulation of the detector and thus validated the analysis. The analysis was further a tool used to numerically optimize performance of the TST when the actual FH SNR deviated from that assumed. In order to study the performance of tests synthesized by assuming an extremely small FH SNR, expressions for the asymptotic test efficiencies were computed. This asymptotic analysis also yielded simplified test parameter expressions applicable to the small SNR case.

A significant feature of the SPRT, exposed by the analysis, is that, with the same error probabilities, an FH waveform with a given SNR can be detected in less than half the time of the corresponding FSS test. This reduction in detection time is especially significant for Low Probability of Intercept (LPI) applications where the transmissions are purposely short. For the pure SPRT, detection time increased whenever the observed SNR differed from that assumed in the test's synthesis; and for SNR's midway between zero and the assumed value, it was even comparable to the corresponding FSS test. The TST significantly improves this anomaly while sacrificing little performance over that of the purely sequential test, and what little performance was lost, was largely regained by the optimal TST. The decrease in the detection time of the sequential tests can be used to robustify the test with respect to the input SNR while maintaining better performance than that of the nonrobust FSS test. The simplified test parameter expressions derived by asymptotic methods may be useful for any schemes to adapt these tests for varying FH SNR's. The three tests and their corresponding design and performance analysis also apply to the slow FH case. The detector structure is suboptimal for slow FH, but it is believed the performance loss is small, especially for detection times that include a large number of hops.

It is apparent that other simplifications and extensions to these results are possible. For instance, it was assumed that the starting time and duration of the chip epoch were known. This first restriction might be relaxed by redefining the SELF to perform sliding window integration instead of the integrate and dump operation now performed. This, of course, would degrade the detector's performance for some values of epoch starting time, but it might exhibit better average performance. There are also possible simplifications to the SELF to improve its implementability. Among these would be the removal of the emphasizing function which would make the detector structure suboptimal, but it would probably still be asymptotically optimal for small assumed SNR's. Another simplification would be coarse subband preselection where the total SS bandwidth is subdivided into subbands, each containing a large number of chip frequencies. An algorithm could then be used to select a subset of the subbands that would most likely contain the intercepted signal. Detailed processing on these preselected bands could then be done with the methods described in this paper.

Appendix

A. Derivation of SELF

Proceeding from Appendix B of [1], the likelihood function, given the carrier phase θ and the channel k, the conditional likelihood function for the ith epoch is

$$\Lambda_i(y/k, \theta) = \exp\left[-\frac{E}{N_0}\right] \exp \frac{2}{N_0} \int_{iT_h}^{(i+1)T_h} y(t)\, x_i(t)\, dt \tag{85}$$

where E is the single-epoch energy of the FH signal, i.e.,

$$E = \int_{iT_h}^{(i+1)T_h} 2S \sin^2(\omega_{k_i} t + \theta)\, dt. \tag{86}$$

But

$$E \approx ST_h \qquad \text{for } \omega_{k_i} T_h \gg 1 \tag{87}$$

which upon substitution into the conditional likelihood function (85) and expanding $x_i(t)$ yields

$$\Lambda_i(y/k, \theta) = e^{-\gamma} e^{\sqrt{2\gamma}(P_k \sin\theta + Q_k \cos\theta)} \tag{88}$$

where

$$P_k = \frac{2}{\sqrt{N_0 T_h}} \int_{iT_h}^{(i+1)T_h} y(t) \cos \omega_{k_i} t\, dt$$

$$Q_k = \frac{2}{\sqrt{N_0 T_h}} \int_{iT_h}^{(i+1)T_h} y(t) \sin \omega_{k_i} t\, dt. \tag{89}$$

Taking expectations with respect to θ defines

$$\Lambda_i(y/k) \triangleq E_\theta[\Lambda_i(y/k, \theta)] \tag{90}$$

which is the likelihood function conditional only on the channel. This expectation can be evaluated as follows:

$$E_\theta[\Lambda_i(y/k, \theta)] = \frac{e^{-\gamma}}{2\pi} \int_0^{2\pi} e^{\sqrt{2\gamma}(P_k \sin\theta + Q_k \cos\theta)}\, d\theta \tag{91}$$

$$= \frac{e^{-\gamma}}{2\pi} \int_0^{2\pi} e^{\sqrt{2\gamma}\sqrt{P_k^2 + Q_k^2} \sin(\theta + \psi)}\, d\theta \tag{92}$$

where $\psi = \operatorname{Arg}(P_k + jQ_k)$. Now by the periodicity of the integrand

$$E_\theta[\Lambda_i(y/k, \theta)] = \frac{e^{-\gamma}}{2\pi} \int_0^{2\pi} e^{\sqrt{2\pi}\sqrt{P_k^2 + Q_k^2} \cos\theta}\, d\theta \tag{93}$$

$$= e^{-\gamma} I_0\left(\sqrt{2\gamma}\sqrt{P_k^2 + Q_k^2}\right) \tag{94}$$

by the identity

$$I_0(a) = \frac{1}{2\pi}\int_0^{2\pi} e^{a\cos\theta}\,d\theta \tag{95}$$

where I_0 is the zeroth-order modified Bessel function of the first kind. Taking expectations with respect to the channel k yields the Single-Epoch Likelihood Function (SELF)

$$\Lambda_i(y) \triangleq E_k[\Lambda_i(y/k)] \tag{96}$$

$$= \frac{e^{-\gamma}}{K}\sum_{k=0}^{K-1} I_0\left(\sqrt{2\gamma}\sqrt{P_k^2 + Q_k^2}\right). \tag{97}$$

B. Asymptotic Expressions of the ALLF Moments

We want to examine the behavior of the ALLF moments when SNR γ diminishes while the relative SNR r is held constant. The asymptotic expressions derived here encapsulate this behavior. To derive asymptotic expressions for the mean and variance of the ALLF, we need only consider the mean and variance, $\mathfrak{M}_r$ and $\mathfrak{V}_r$, respectively, of the single-epoch ALLF. To this end, it will be useful to derive asymptotic expression of two functions of the channel moments: μ_r/σ_0 and σ_r^2/σ_0^2. Starting with the first expression and substituting (23) and (24), we obtain

$$\frac{\mu_r^2}{\sigma_0^2} = \frac{I_0^2(2r\gamma)}{[I_0(2\gamma) - 1]}. \tag{98}$$

We will need a partial power series expansion of $I_0(x)$, i.e.,

$$I_0(x) = 1 + \frac{x^2}{4} + \frac{x^4}{64} + \mathcal{O}(x^6). \tag{99}$$

Here and throughout this discussion, the quantity $\mathcal{O}(x^n)$ represents any function, say $f(x)$, such that

$$x^{-n}\lim_{x\to 0} f(x) < \infty. \tag{100}$$

The particular function represented by $\mathcal{O}(x^n)$ is determined from the context of the equation in which it appears. With the above power series for I_0, (98) becomes

$$\frac{\mu_r^2}{\sigma_0^2} = \frac{[1 + r^2\gamma^2 + \mathcal{O}(\gamma^4)]^2}{\gamma^2 + \frac{1}{4}\gamma^4 + \mathcal{O}(\gamma^6)} \tag{101}$$

$$= \frac{1 + 2r^2\gamma^2 + \mathcal{O}(\gamma^4)}{\gamma^2 + \frac{1}{4}\gamma^4 + \mathcal{O}(\gamma^6)} \tag{102}$$

$$= \gamma^{-2} + (2r^2 - \tfrac{1}{4}) + \mathcal{O}(\gamma^2) \tag{103}$$

$$= [\gamma^{-1} + (r^2 - \tfrac{1}{8})\gamma + \mathcal{O}(\gamma^3)]^2 \tag{104}$$

thus,

$$\frac{\mu_r}{\sigma_0} = \gamma^{-1} + (r^2 - \tfrac{1}{8})\gamma + \mathcal{O}(\gamma^3). \tag{105}$$

Now to evaluate the second channel moment function. Using (23) and (99), plus the power series for e^x, we get after carrying out the multiplications

$$\frac{\sigma_r^2}{\sigma_0^2} = [I_0(2\gamma) - 1]^{-1}\left[\frac{1}{\pi}\int_0^{\pi} e^{-2\gamma\cos\phi} I_0\left(4r\gamma\sin\frac{\phi}{2}\right)d\phi - I_0^2(2r\gamma)\right] \tag{106}$$

$$\frac{\sigma_r^2}{\sigma_0^2} = \left[\gamma^2 + \frac{1}{4}\gamma^4 + \mathcal{O}(\gamma^6)\right]^{-1} \cdot \left\{\frac{1}{\pi}\int_0^{\pi}\left[1 - 2\gamma\cos\phi + 2\gamma^2\cos^2\phi - \frac{4}{3}\gamma\cos^3\phi^3 + \frac{2}{3}\cos^4\phi\gamma^4 + \mathcal{O}(\gamma^5)\right] \times \left[1 + 4r^2\gamma^2\sin^2\frac{\phi}{2} + 4r^4\gamma^4\sin^4\frac{\phi}{2} + \mathcal{O}(\gamma^6)\right]d\phi - \left[1 + r^2\gamma^2 + \frac{1}{4}r^4\gamma^4 + \mathcal{O}(\gamma^6)\right]^2\right\} \tag{107}$$

$$\frac{\sigma_r^2}{\sigma_0^2} = \left[\gamma^2 + \frac{1}{4}\gamma^4 + \mathcal{O}(\gamma^6)\right]^{-1}\left\{\frac{1}{\pi}\int_0^{\pi}\left[1 - 2\cos\phi\gamma + \left(4r^2\sin^2\frac{\phi}{2} + 2\cos^2\phi\right)\gamma^2 - \left(8r^2\cos\phi\sin^2\frac{\phi}{2} + \frac{4}{3}\cos^3\phi\right)\gamma^3 + \left(\frac{2}{3}\cos^4\phi + 8r^2\cos^2\phi\sin^2\frac{\phi}{2} + 4r^4\sin^4\frac{\phi}{2}\right)\gamma^4 + \mathcal{O}(\phi, \gamma^5)\right]d\phi - \left[1 + 2r^2\gamma^2 + \frac{3}{2}r^4\gamma^4 + \mathcal{O}(\gamma^6)\right]\right\}. \tag{108}$$

Let $f(\phi, \gamma^5)$ be the particular function represented by the symbol $\mathcal{O}(\phi, \gamma^5)$ under the integral, then

$$\lim_{\gamma\to 0}\gamma^{-5}\int_0^{\pi} f(\phi, \gamma^5) = \int_0^{\pi}\lim_{\gamma\to 0}\gamma^{-5} f(\phi, \gamma^5) < \infty \tag{109}$$

implying that $\int_0^{\pi} f(\phi, \gamma^5) \in \mathcal{O}(\gamma^5)$. The interchange of the limit and integration is justified as follows. The function $f(\phi, \gamma^5)$ inherits continuity on the compact set $\{\phi, \gamma : \phi \in [0, \pi]$ and $\gamma \in [0, 1]\}$ from the integrand of which it is a component. Therefore, $\gamma^{-5} f(\phi, \gamma^5)$, which has a finite limit at the origin, is also continuous on this compact set and hence is bounded, say by B, on this set. The function B is integrable on $\phi \in [0, \pi]$ by which the interchange follows by the Lebesgue Dominated Convergence theorem. The interchange implies that (108) can be

integrated termwise to yield

$$\frac{\sigma_r^2}{\sigma_0^2} = \left[\gamma^2 + \tfrac{1}{4}\gamma^4 + \mathcal{O}(\gamma^6)\right]^{-1} \times \left\{\left[1 + (2r^2+1)\gamma^2 + 2r^2\gamma^3 + (\tfrac{1}{4} + 2r^2 + \tfrac{3}{2}r^4)\gamma^4 + \mathcal{O}(\gamma^5)\right] - \left[1 + 2r^2\gamma^2 + \tfrac{3}{2}r^4\gamma^4 + \mathcal{O}(\gamma^6)\right]\right\} \quad (110)$$

which simplifies to

$$\frac{\sigma_r^2}{\sigma_0^2} = 1 + 2r^2\gamma + 2r^2\gamma^2 + \mathcal{O}(\gamma^3). \quad (111)$$

With these asymptotic expressions for μ_r/σ_0 and σ_r^2/σ_0^2, we proceed with the derivation of asymptotic expressions for the ALLF moments. The ALLF mean is expressed in terms of the SELF moments as

$$\mathfrak{M}_r = \frac{1}{2}\ln\frac{V_0}{V_1} + [2V_1V_0]^{-1}\left\{[M_r - M_0]^2V_1 - [M_r - M_1]^2V_0 + [V_1 - V_0]V_r\right\}. \quad (112)$$

The last three terms can be evaluated as follows:

$$[2V_1V_0]^{-1}\left\{[M_r - M_0]^2V_1 - [M_r - M_1]^2V_0 + [V_1 - V_0]V_r\right\}$$

$$= \frac{1}{2K}\left[K - 1 + \frac{\sigma_1^2}{\sigma_0^2}\right]^{-1}\left\{\left[\frac{\mu_r}{\sigma_0} - \frac{\mu_0}{\sigma_0}\right]^2 \cdot \left[K - 1 + \frac{\sigma_1^2}{\sigma_0^2}\right] - K\left[\frac{\mu_r}{\sigma_0} - \frac{\mu_1}{\sigma_0}\right]^2 + \left[K - 1 + \frac{\sigma_r^2}{\sigma_0^2}\right]\left[\frac{\sigma_1^2}{\sigma_0^2} - 1\right]\right\} \quad (113)$$

$$= \frac{1}{2K}\left[K + 2\gamma + \mathcal{O}(\gamma^2)\right]^{-1}\left\{\left[r\gamma + \mathcal{O}(\gamma^3)\right]^2 \cdot \left[K + \mathcal{O}(\gamma)\right] - K\left[(r^2-1)\gamma + \mathcal{O}(\gamma^3)\right]^2 + \left[K + 2r^2\gamma + \mathcal{O}(\gamma^2)\right]\left[2\gamma + 2\gamma^2 + \mathcal{O}(\gamma^3)\right]\right\} \quad (114)$$

$$= \frac{\gamma}{K} + \left(\frac{K+2}{K^2}r^2 + \frac{K-4}{2K^2}\right)\gamma^2 + \mathcal{O}(\gamma^3). \quad (115)$$

Now for the final term. We will need the following power series expansion for $\ln(x)$:

$$\ln(1+x) = x - \frac{x^2}{2} + \mathcal{O}(x^3) \quad (116)$$

$$\frac{1}{2}\ln\left(\frac{V_0}{V_1}\right) = -\frac{1}{2}\ln\left[1 - \frac{1}{K} + \frac{1}{K}\frac{\sigma_1^2}{\sigma_0^2}\right] \quad (117)$$

$$= -\frac{1}{2}\ln\left[1 + \frac{2}{K}\gamma + \frac{2}{K}\gamma^2 + \mathcal{O}(\gamma^3)\right] \quad (118)$$

$$= -\frac{\gamma}{K} + \left(\frac{1}{K^2} - \frac{1}{K}\right)\gamma^2 + \mathcal{O}(\gamma^3) \quad (119)$$

combining (115) and (119)

$$\mathfrak{M}_r = \frac{K+2}{K^2}\left(r^2 - \frac{1}{2}\right)\gamma^2 + \mathcal{O}(\gamma^3). \quad (120)$$

Now to proceed with the variance.

$$\mathfrak{V}_r = \frac{V_r^2}{2}\left(\frac{1}{V_0} - \frac{1}{V_1}\right)^2 + \left[\left(\frac{1}{V_0} - \frac{1}{V_1}\right)M_r + \left[\frac{M_1}{V_1} - \frac{M_0}{V_0}\right]\right]^2 V_r. \quad (121)$$

The first term can be evaluated as

$$\frac{V_r^2}{2}\left(\frac{1}{V_0} - \frac{1}{V_1}\right)^2 = \frac{1}{2K^2}\left\{\frac{\left[\frac{\sigma_1^2}{\sigma_0^2} - 1\right]\left[K - 1 + \frac{\sigma_r^2}{\sigma_0^2}\right]}{\left[K - 1 + \frac{\sigma_1^2}{\sigma_0^2}\right]}\right\}^2 \quad (122)$$

$$= \frac{1}{2K^2}\left\{\frac{[2\gamma + \mathcal{O}(\gamma^2)][K + \mathcal{O}(\gamma)]}{[K + \mathcal{O}(\gamma)]}\right\}^2 \quad (123)$$

$$= \frac{2\gamma^2}{K^2} + \mathcal{O}(\gamma^3). \quad (124)$$

The second term of (121)

$$\left[\left(\frac{1}{V_0} - \frac{1}{V_1}\right)M_r + \left[\frac{M_1}{V_1} - \frac{M_0}{V_0}\right]\right]^2 V_r = \frac{1}{K^2}\frac{\left[K - 1 + \frac{\sigma_r^2}{\sigma_0^2}\right]}{\left[K - 1 + \frac{\sigma_1^2}{\sigma_0^2}\right]^2}\left\{\left[\frac{\sigma_1^2}{\sigma_0^2} - 1\right] \cdot \left[(K-1)\frac{\mu_0}{\sigma_0} + \frac{\mu_r}{\sigma_0}\right] + K\left[\frac{\mu_1}{\sigma_0} - \frac{\mu_0}{\sigma_0}\frac{\sigma_1^2}{\sigma_0^2}\right]\right\}^2 \quad (125)$$

$$= \frac{1}{K^2}\frac{[K + \mathcal{O}(\gamma)]}{[K + \mathcal{O}(\gamma)]^2}\left\{[2\gamma + 2\gamma^2 + \mathcal{O}(\gamma^3)] \cdot [K\gamma^{-1} + \mathcal{O}(\gamma)] + K\left[\gamma^{-1} + \frac{7}{8}\gamma + \mathcal{O}(\gamma^3)\right] - K\left[\gamma^{-1} - \frac{1}{8}\gamma + \mathcal{O}(\gamma^3)\right] \cdot [1 + 2\gamma + 2\gamma^2 + \mathcal{O}(\gamma^3)]\right\}^2 \quad (126)$$

$$= \frac{1}{K^2}\frac{[K + \mathcal{O}(\gamma)]}{[K + \mathcal{O}(\gamma)]^2}\left\{[2K + 2K\gamma + \mathcal{O}(\gamma^2)] + K[-2 - \gamma + \mathcal{O}(\gamma^2)]\right\}^2 \quad (127)$$

$$= \frac{\gamma^2}{K} + \mathcal{O}(\gamma^3). \quad (128)$$

Combining (124) and (128) yields

$$\mathcal{V}_r = \frac{K+2}{K^2}\gamma^2 + \mathcal{O}(\gamma^3). \quad (129)$$

Summarizing these results:

$$\mathfrak{M}_r = \frac{K+2}{K^2}\left(r^2 - \frac{1}{2}\right)\gamma^2 + \mathcal{O}(\gamma^3) \quad (130)$$

$$\mathcal{V}_r = \frac{K+2}{K^2}\gamma^2 + \mathcal{O}(\gamma^3). \quad (131)$$

References

[1] D. G. Woodring, "Performance of optimum and suboptimum detectors for spread spectrum waveforms," Naval Res. Lab., Washington, DC, Tech. Rep. 8432, Dec. 1980.

[2] J. D. Edell, "Wideband, noncoherent, frequency-hopped waveforms and their hybrids in low-probability-of-intercept communications," Naval Res. Lab., Washington, DC, Tech. Rep. 8025, Nov. 1976.

[3] A. Wald, *Sequential Analysis*. New York: Wiley, 1947.

[4] N. Shiryayev, *Optimal Stopping Rules*. New York: Springer-Verlag, 1977.

[5] D. A. Darling and A. J. F. Siegert, "The first passage problem for a continuous Markov process," *Ann. Math. Stat.*, vol. 24, pp. 624–639, 1953.

[6] T. W. Anderson, "A modification of the sequential probability ratio test to reduce the sample size," *Ann. Math. Stat.*, vol. 31, pp. 165–197, 1960.

[7] S. Tantaratana and H. V. Poor, "Asymptotic efficiencies of truncated sequential tests," *IEEE Trans. Inform. Theory*, vol. IT-28, pp. 911–923, Nov. 1982.

[8] S. Tantaratana and J. B. Thomas, "Truncated sequential probability ratio test," *Inform. Sci.*, vol. 13, pp. 283–300, 1977.

[9] G. N. Watson, *A Treatise on the Theory of Bessel Functions*. New York: Cambridge University Press, 1980.

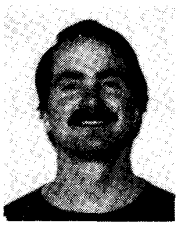

William E. Snelling received the bachelor's and master of science degrees in electrical engineering from the Georgia Institute of Technology in 1979 and 1980, respectively. He is currently completing the Ph.D. dissertation at the University of Maryland.

Between 1980 and 1981 he was a Teaching Assistant at the Georgia Institute of Technology. Since 1981 he has been with the Johns Hopkins University, Applied Physics Laboratory, where he is currently a Senior Staff Engineer involved in signal processing systems for Doppler fire-control radars. His signal processing activities concern algorithm analysis and development, especially of the highly concurrent type, and their implementation using specialized processors and custom VLSI and VHSIC technology. He is also interested in interception and exploitation of secure communications.

Mr. Snelling is a member of Tau Beta Pi.

Evaggelos Geraniotis (S'76–M'82–SM'88) was born in Athens, Greece, on July 8, 1955. He received the Diploma in electrical engineering from the National Technical University of Athens, Athens, Greece, in 1978, and the M.S. and Ph.D. degrees in electrical engineering from the University of Illinois at Urbana-Champaign in 1980 and 1983, respectively.

From August 1978 to June 1982 he was a Research Assistant at the Coordinated Science Laboratory, University of Illinois. From September 1982 to August 1985 he was an Assistant Professor of Electrical and Computer Engineering at the University of Massachusetts, Amherst. Since September 1985 he has been with the University of Maryland, College Park, where he is presently an Associate Professor of Electrical Engineering and a member of the Systems Research Center. His research has been in communication theory, information theory, and their applications with current emphasis on spread-spectrum and antijam communications, multiuser communications, radio networks, robust and distributed detection, estimation and filtering, error-control coding, and digital signal processing. He is the author of over 60 technical papers in these areas in journals and conference proceedings. He serves regularly as a consultant in the areas of spread-spectrum and antijam systems, protocols for packet radio networks, radar systems, robust chaff-target discrimination, and interception and feature detection for governmental and industrial clients. In the past two years he has served as Program Chairman and Treasurer/Secretary of the Washington DC/Northern Virginia Chapter of the Information Theory Group and is currently its Vice Chairman.

Dr. Geraniotis is a member of Phi Kappa Phi, Tau Beta Pi, Eta Kappa Nu, and the Technical Chamber of Greece. Since February 1989 he has been serving as the Editor for Spread Spectrum of the IEEE TRANSACTIONS ON COMMUNICATIONS.